XXXI Seminarium

ZASTOSOWANIE KOMPUTERÓW W NAUCE I TECHNICE 2021

Oddział Gdański PTETiS

doi: 10.32016/1.73.05

DETECTION OF PETROLEUM PRODUCTS USING OPTICAL COHERENCE TOMOGRAPHY

Aleksandra M. KAMIŃSKA[1], **Jerzy PLUCIŃSKI**[2]

1. Gdańsk University of Technology, Faculty of Electronics, Telecommunications and Informatics
   tel.: +48 58 347 2642 e-mail: aleksandra.kaminska@pg.edu.pl
2. Gdańsk University of Technology, Faculty of Electronics, Telecommunications and Informatics
   tel.: +48 58 347 2642 e-mail: pluc@eti.pg.edu.pl

Abstract: In this work, we present a novel method developed for the analysis of the properties of thin layers for detecting petroleum products on a water surface using a commercially available optical coherence tomography (OCT) system. The spectral density analysis of the signal from a spectroscopic OCT (S-OCT) enables us to perform the precision calculation of the thin layer thickness and other properties like homogeneity, and dispersion, even if layer thickness is smaller than the coherence length of light from the used broadband light source. Mathematical modeling has been confirmed by measurements. The experiment with thin oil films on the surface of the water was conducted. The obtained results indicate that it is possible to measure the thickness of the petroleum product layers on the surface of the water smaller than 1 μm with 10 nm resolution.

Keywords: pollutions, petroleum products, detection, optical coherence tomography.

1. INTRODUCTION

Petrochemical waste can be damaging or lethal to aquatic organisms even in small concentrations [1]. Water-insoluble phases can be readily detected by interferometric methods due to the difference between refractive indices of water and oils. Their presence can signal the need for more detailed chemical analysis, thus saving time and resources.

The thickness of the thin layer of oil on the surface of water can be measured using low-coherence interferometry (LCI), in particular case optical coherence tomography (OCT), which joins longitudinal scanning by the LCI and transverse beam scanning to obtain three-dimensional images of the object under test. A diagram of the OCT measuring system is shown in Figure 1.

Standard OCT systems image the internal structure of the examined object in the longitudinal direction by measuring the difference in optical path lengths that optical radiation propagates in the measuring arm, in which the examined object is located, and in the reference arm, at the end of which the mirror is located. If the reflection in the examined object from features located at different depths takes place, then these depths can be distinguished if they differ by a value greater than the coherence length of the optical radiation source used. For this reason, OCT systems use sources with a very short coherence path length, i.e., with a very wide spectrum (broadband sources).

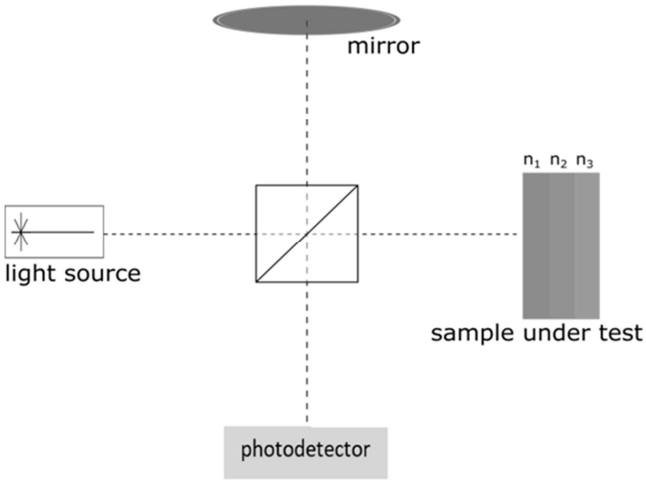

Fig. 1. OCT system diagram

Measurement of the depth at which the optical signal is reflected or backscattered in the sample under test is made by analyzing the signal at the output of the OCT system interferometer measured by a photodetector located at its output. If the mirror moves in the reference arm during measurement, a photodiode is used as the photodetector. This method is used by time-domain OCT (TD-OCT) systems. The alternative is fixed mirror systems used by Fourier-domain (FD-OCT) systems. The FD-OCT systems need a spectrometer working as the photodetector spectral-domain OCT. This method is used by spectral-domain (SD-OCT) systems SD-OCT). The spectrometer is not needed when a tunable laser source is used as the light source. This method is used by the latest generation of OCT systems, i.e., by swept-source OCT (SS-OCT) systems.

The main obstacle to measurements of oil layers on the water surface by OCT is inadequate axial resolution. A marine oil spill with a quantity spread as much as 19.463 L/ha results in a layer of oil only 2.0320 μm thick [2], while the measurement resolution of the layer thickness of the typical OCT system equals about 10 μm [3]. However, a layer of oil of thickness within the coherence length of light used in measurement causes thin-film interference due to multiple Fresnel reflections on the oil-air and oil-water interfaces. This effect can be utilized to detect layers of thickness significantly smaller than the resolution of the measurement setup.

2. MATHEMATICAL MODELING

The mathematical model of the OCT system for measurement of thin layers is based on modeling of two interferometers: a Fabry-Pérot interferometer for modeling the light propagation in a thin layer and a Michelson interferometer for modeling the OCT system (see Figure 2) [4]. By modeling the propagation of optical radiation within the layer, the amplitude spectral density of the wave reflected from it in the measurement arm of the Michelson interferometer can be calculated [5, 6].

a)

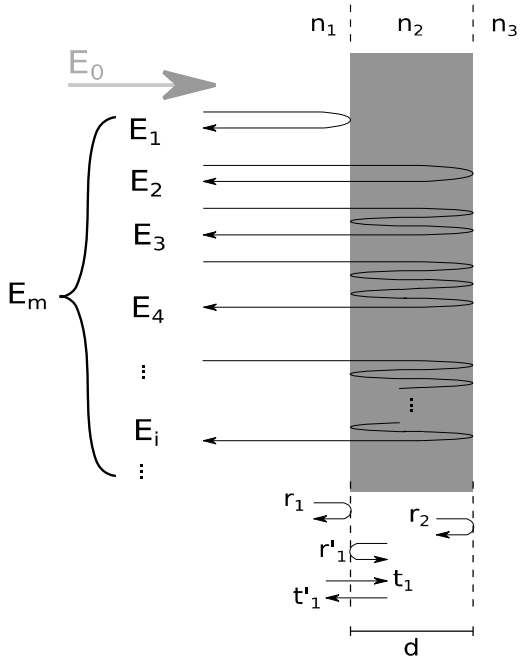

b)

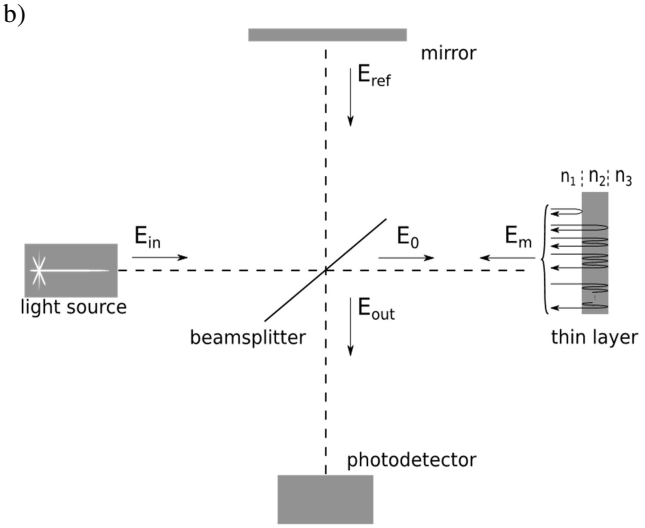

Fig. 2. Modeling of the propagation of optical radiation inside the layer (a) and in the measuring interferometer of the OCT system (b)

Since the Gaussian beam propagation is modeled inside the layer with a thickness much smaller than the Rayleigh range of the beam, the influence of the Gouy effect phenomenon and the expansion of the beam during propagation in the layer on the amplitude of the reflected wave can be neglected in the calculations [7]. In this case, the complex amplitude E_m of the beam reflected from the layer can be obtained as the sum of the infinite number of the complex amplitudes E_1, E_2,… of the reflected waves from the boundaries between the layer and air or water (see Figure 2a):

$$E_{\mathrm{m}} = \sum_{i=1}^{\infty} E_i , \tag{1}$$

where

$$E_i = \begin{cases} r_1 E_0 & , \text{if } i = 1 \\ (r'_1)^{i-2} r_2^{i-1} t_1 t'_1 \exp[-j4\pi(i-1)n_2 d/\lambda] E_0, & \text{if } i > 1 \end{cases}, \tag{2}$$

and where E_0 is the complex amplitude of incident beam, d and n_2 are the thickness and the refractive index of the layer, respectively, r_1, r'_1, and r_2 are the reflection coefficients, t_1 and t'_1 are the transmission coefficients (see Figure 2a) that can be obtained from Fresnel equations:

$$r_1 = \frac{n_1 - n_2}{n_1 + n_2}, \tag{3}$$

$$r'_1 = \frac{n_2 - n_1}{n_1 + n_2} = -r_1, \tag{4}$$

$$r_2 = \frac{n_2 - n_3}{n_2 + n_3}, \tag{5}$$

$$t_1 = 1 + r_1 , \tag{6}$$

$$t'_1 = 1 + r'_1 = 1 - \mathrm{r}_1, \tag{7}$$

where n_1 and n_3 are the refractive indexes of the media in front and behind the layer.

Noting that for $i > 1$, the amplitudes E_i form a geometric sequence, from Equation (1) we obtain [4]:

$$E_{\mathrm{m}} = \left[r_1 + \frac{(1 - r_1^2) r_2 \exp(-j4\pi n_2 d/\lambda)}{1 + r_1 r_2 \exp(-j4\pi n_2 d/\lambda)} \right] E_0. \tag{8}$$

The intensity I_{out} of the output beam from the Michelson's interferometer of the OCT system is equal to the average square of the module of the complex amplitude E_{out} of the beam. Since this amplitude is equal to the sum of the complex amplitudes E'_{m} and E'_{ref} of beams coming from measurement and reference arms and guided by the beamsplitter to the detector (see Figure 2b), we obtain:

$$I_{\mathrm{out}}(\lambda) = \langle |E_{\mathrm{out}}|^2 \rangle = \langle |E'_{\mathrm{m}} + E'_{\mathrm{ref}}|^2 \rangle. \tag{9}$$

For lossless beamsplitter, from Equation (1) and Relationship (9), we finally obtain:

$$I_{\mathrm{out}}(\lambda) = \\ = \frac{1}{4} \left\langle \left| r_1 + \frac{(1 - r_1^2) r_2 \exp(-j4\pi n_2 d/\lambda)}{1 + r_1 r_2 \exp(-j4\pi n_2 d/\lambda)} + \exp(j2\pi \Delta z/\lambda) \right|^2 \right\rangle I_{\mathrm{i}\square}(\lambda), \tag{10}$$

where Δz is the difference in the optical path length of interfering beams from the measurement and reference arms of Michelson's interferometer and $I_{\mathrm{i}\square}$ is the intensity of the input beam directed from the light source to the beam splitter.

Equation (10) allows us to obtain the power spectral density at the output of the OCT system for a layer with a given thickness and refractive index. This equation can be used in a method that will make it possible to measure the thickness of a layer with a thickness less than the coherence

path length of the light source and its dispersion based on the measured signal spectrum at the output of the OCT system interferometer. This can be done by using the method of fitting the data obtained from mathematical modeling, with different set parameters of the layer, to the measurement data, using an optimization method in which the objective function will be to achieve a minimum global difference between these data.

3. MEASUREMENTS

In the measurement experiment, engine oil with a refractive index of 1.47 was used. Small amounts of this oil were pipetted onto the surface of distilled water placed in a Petri dish, which resulted in the formation of a thin layer on this surface (see Figure 3). These oil layers were then measured using the SS-OCT system with commercial laser swept source HSL-2000 (by Santec, Japan). Detailed parameters of the system are presented in Table 1.

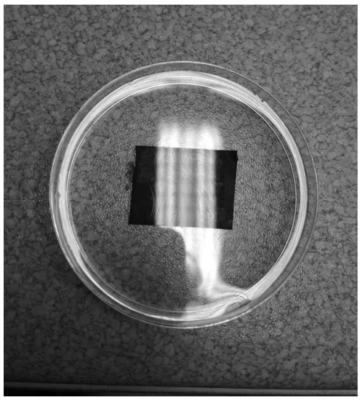

Fig. 3. A thin layer on a surface of distilled water placed in a Petri dish (the dark rectangle under the dish makes it easier to observe the formation of rainbow patterns on this surface after the layer is formed)

Table 1. Parameters of the SS-OCT system.

Item	Value
Light source type	Diode laser – 20 kHz swept source
Output power of the laser	10 mW
Central wavelength	1320 nm
Wavelength range	140 nm
Longitudinal resolution	12 µm
Lateral resolution	15 µm
Frame rate	> 4 fps
Depth imaging range	7 mm
Transverse imaging range	10 mm

Measurements of normalized power spectral density of the optical signal at the output of measurement interferometer of the OCT system for several layers of oil of different thicknesses are shown in Figures 4–6. The same figures show the densities calculated with the use of mathematical modeling obtained for a source with the homogeneous spectral distribution. In the modeling process, the goal function was to minimize the difference of carrier periods of the calculated and measured normalized power spectral densities and the position differences of the minima and maxima of envelopes of these densities. Mathematical modeling allowed us to estimate the thickness of the oil layer, which for subsequent samples was 3.16 µm, 3.75 µm, and 6.02 µm.

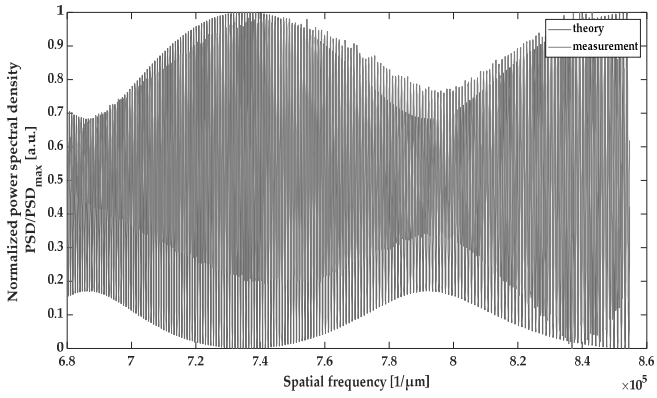

Fig. 4. Normalized power spectral density of the optical signal at the output of measurement interferometer of the OCT system for the layer of oil – the thickness of layer 3.16 µm

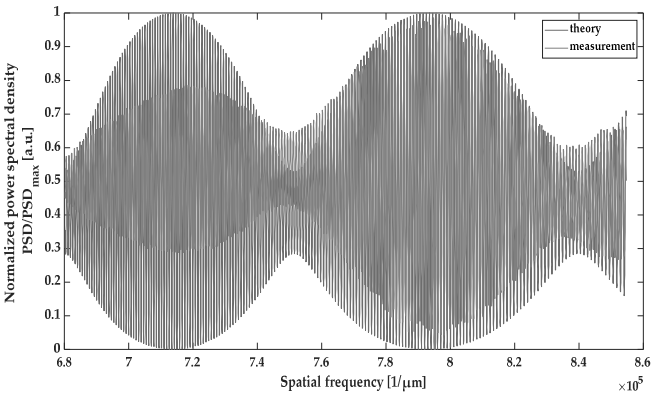

Fig. 5. Normalized power spectral density of the optical signal at the output of measurement interferometer of the OCT system for the layer of oil – the thickness of layer 3.75 µm

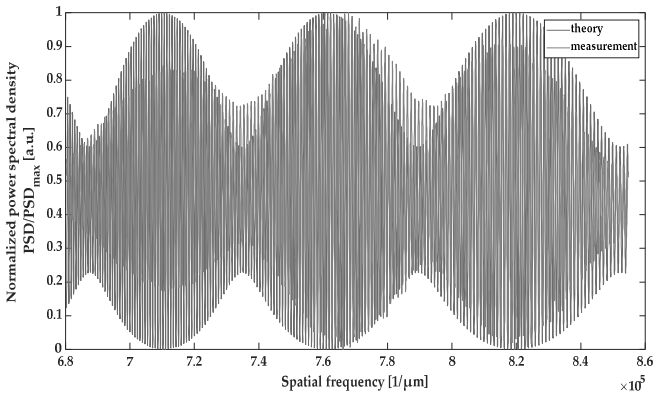

Fig. 6. Normalized power spectral density of the optical signal at the output of measurement interferometer of the OCT system for the layer of oil – the thickness of layer 6.02 µm

The calculated normalized power spectral densities presented in Figures 4–6 differ from the measured ones. There are several reasons for this: 1) the used source did not have flat power spectral density, 2) the chromatic aberration of the lens in the measurement system caused the location of the waist of the scanning beam to change its position as a function of the wavelength, which resulted in noticeable changes in the intensity of the radiation reflected from the measured layer, 3) the sampling frequency in the spatial

frequency domain slightly differed from the linear one in the spectrum range of the used laser (this causes the unequal period of the strips generated by the Moiré phenomenon when the calculated and measured power spectral densities are superimposed on each other in Figures 4–6). In further research, a better, higher accuracy wavelength measurement method will be employed along with the use of a suitable windowing function (e.g. Gaussian) to obtain a better agreement of the measured and calculated power spectral densities.

4. CONCLUSIONS

The reflectivity of the surface of water changes in the presence of a thin layer of petrochemical substance on the surface. This phenomenon can be used in the detection of petroleum contamination with interferometric techniques. Presented simulation and measurement results show that optical low-coherence interferometry, including optical coherence tomography with spectroscopic detection, can be used to detect the presence and to measure the thickness of these layers. The presented measurement results were obtained on the OCT system that was not designed to measure layers with a thickness smaller than the coherence length path of the radiation source used. It should be noted that the OCT system was able to measure layers about four times thinner than the two-point longitudinal resolution of it, which makes the proposed method unique. The same method can be used for the measurement of thin layers by OCT systems using a source with a wider spectrum and a shorter central wavelength. Such sources allow the construction of OCT systems with a sub-micrometer two-point longitudinal resolution [8–11]. Lu H. *et. al* showed that optical reflectometry techniques allow us to measure thin layer thicknesses with a resolution of 12 nm [12]. Therefore, it should be expected that after careful calibration of the OCT system with such a source and using the proposed method the oil-derivative layers of thickness significantly thinner than 1 μm will be possible to detect and their thickness will be measurable with resolution better than 10 nm.

5. REFERENCES

1. Pacheco M., Santos M.A.: Biotransformation, Endocrine, and Genetic Responses of Anguilla anguilla L. to Petroleum Distillate Products and Environmentally Contaminated Waters. Ecotoxicology and Environmental Safety, vol. 49, 2001, pp. 64-75.
2. Tchobanoglous G., Burton F.L., Stensel, D.H.: "Chapter 2: Constituents in Wastewater – Oil and Grease" in Wastewater Engineering: Treatment and Reuse, 4th Ed. Metcalf & Eddy Inc., 2003, p. 98.
3. Fujimoto J., Drexler W.: "Chapter 1: Introduction to Optical Coherence Tomography" in Drexler W., Fujimoto J. (Eds.): Optical Coherence Tomography. Springer-Verlag, Berlin Heidelberg, 2008, pp. 1–45.
4. Kamińska A.M., Strąkowski M.R., Pluciński J.: Spectroscopic Optical Coherence Tomography for Thin Layer and Foil Measurements. Sensors, vol. 20, 2020, pp. 5553-1–19.
5. Pluciński J., Karpienko K.: Fiber-optic Fabry-Pérot sensors – modeling versus measurements results. Proc. SPIE, vol. 10034, 2016, pp. 100340H-1–7.
6. Pluciński J., Karpienko K.: Response of a fiber-optic Fabry-Pérot interferometer to refractive index and absorption changes – modeling and experiments. Proc. SPIE, vol. 10161, 2016, pp. 101610F-1–7.
7. Saleh B.E.A, Teich M.C.: Fundamentals of Photonics, 3rd Ed. John Wiley & Sons, 2019, pp. 80–88.
8. Boris Povazay, Alexander A. Apolonski, Angelika Unterhuber, Boris Hermann, Kostadinka K. Bizheva, Harald Sattmann, Phillip St. J. Russell, Ferenc Krausz, Adolf Friedrich Fercher, Wolfgang Drexler: Visible light optical coherence tomography. Proc. SPIE, vol. 4619, 2002, pp. 90–94.
9. Czajkowski J., Prykäri T., Alarousu E., Palosaariet J., Myllylä R.: Optical coherence tomography as a method of quality inspection for printed electronics products. Opt. Rev., vol. 27, 2010, pp. 257–262.
10. Czajkowski J., Fabritius T., Ułański J., Marszałek T., Gazicki-Lipman M., Nosal A., Śliż R., Alarousu E., Prykäri T., Myllylä R., Jabbour G.: Ultra-high resolution optical coherence tomography for encapsulation quality inspection. Appl. Phys. B, vol. 105, 2011, pp. 649–657.
11. Bizheva K, Tan B., MacLelan B., Kralj O., Hajialamdari M., Hileeto D., Sorbara L.: Sub-micrometer axial resolution OCT for in-vivo imaging of the cellular structure of healthy and keratoconic human corneas. Biomed. Opt. Express, vol. 8, 2017, pp. 800–812.
12. Lu H., Wang M.R., Wang J., Shen M.: Tear film measurement by optical reflectometry technique. J. Biomed. Opt., vol. 19, 2014, pp. 027001-1–9.

WYKRYWANIE PRODUKTÓW NAFTOWYCH ZA POMOCĄ OPTYCZNEJ TOMOGRAFII KOHERENCJI

W pracy przedstawiono nowatorską metodę analizy właściwości cienkich warstw przy użyciu standardowych dostępnych na rynku systemów optycznej tomografii koherentnej (ang. optical coherence tomography – OCT) na potrzeby wykrywania produktów naftowych na powierzchni wody. Analiza gęstości widmowej mocy sygnału pochodzącego z systemu OCT z detekcją spektroskopową (ang. spectroscopic OCT – S-OCT) pozwala na dokładne obliczenie grubości cienkiej warstwy i innych jej właściwości, takich jak jednorodność i dyspersja, nawet jeśli grubość warstwy jest mniejsza niż długość drogi koherencji stosowanego szerokopasmowego źródła światła. Wyniki działania systemu uzyskane metodą modelowania matematycznego zostały potwierdzone pomiarami uzyskanymi z komercyjnego systemu, wykorzystując zaawansowane metody przetwarzania sygnałów. Przeprowadzono eksperyment z cienkimi warstwami olejowymi na powierzchni wody. Na podstawie uzyskanych wyników można stwierdzić, że możliwy jest pomiar grubości warstwy produktu ropopochodnego na powierzchni wody cieńszej niż 1 μm przy rozdzielczości pomiarów 10 nm.

Słowa kluczowe: zanieczyszczenia, produkty ropopochodne, detekcja, optyczna tomografia koherentna.